

**SYNTHESIS AND PROPERTIES OF HIGHLY
CROSS-LINKED POLYSILOXANE FOR
LED ENCAPSULANT**

LOOI YIEN TYNG

UNIVERSITI SAINS MALAYSIA

2012

**SYNTHESIS AND PROPERTIES OF HIGHLY CROSS-LINKED
POLYSILOXANE FOR LED ENCAPSULANT**

by

LOOI YIEN TYNG

Thesis submitted in fulfillment of the requirements

for the degree of

Master of Science

JUNE 2012

ACKNOWLEDGEMENT

I would like to take this opportunity to express my heartiest thanks and deep gratitude to my supervisor, Assoc. Prof. Dr. Zulkifli bin Ahmad for his valuable advice, guidance, encouragement and inspiration throughout the period of this project. His thoughtfulness deeply motivated me throughout this research process. I have learnt a lot on synthesis techniques, result and data interpretations and the most important is self-management and planning. Sincere thanks for his encouragement and help provided from time to time.

Correspondingly, my special thanks to School of Materials & Mineral Resources Engineering, Universiti Sains Malaysia (USM) which has provided a wonderful environment for my research work. I would like to acknowledge the financial assistance of the USM throughout the Research University (RU) Grant and USM Research Fellowship. Acknowledgement is also to be granted to all the assistance and technical staffs in School of Materials & Mineral Resources Engineering, USM for their support from materials processing to testing stage.

Sincere thanks are also extended to all the lecturers in School of Materials & Mineral Resources Engineering, USM especially from the Polymer Engineering Section for their assistance towards the success of this undertaking. My thanks to all the assistance and services from Institute of Postgraduate Studies, library and computer facilities in USM are acknowledgement.

Special acknowledgement is accorded to Prof. Dr. Ahmad Fauzi b. Mohd Noor, Dean of School of Materials & Mineral Resources Engineering and Prof. Dr. Zainal Arifin Mohd Ishak from Department of EITD for granting and helping out in this study.

I am very thankful to my friends, Tay Hong Kang, Mohamad Bisrul, Mohamad Riduan, Rafiza, Law Theng Theng, Lim Su Rong, Chang Lee Nah, Lee Jomay, Lee Jih Houh, Tham Wei Ling and Phua Yi Jing, who always gives me moral support and helps to succeed this work. My acknowledgement to the assistance and inspiration of all the people whomever had offered help directly or indirectly, but thanks must be offered for their cooperation and constructive criticism which help make this thesis reality.

Finally, I would like to dedicate this dissertation to my lovely family and boy friend. Their encouragement, motivation, understanding and care are certainly appreciated.

TABLE OF CONTENTS

ACKNOWLEDGEMENTS	ii
TABLE OF CONTENTS	iv
LIST OF TABLES	ix
LIST OF FIGURES	xi
LIST OF ABBREVIATIONS	xvii
LIST OF SYMBOLS	xix
ABSTRAK	xxi
ABSTRACT	xxii
CHAPTER 1: INTRODUCTION AND PROBLEM STATEMENT	
1.1 Introduction	1
1.2 Problem Statement	3
1.3 Research Objectives	4
CHAPTER 2: LITERATURE REVIEW	
2.1 Light Emitting Diode	5
2.1.1 Introduction	5
2.1.1.1 LED Encapsulant	5
2.2 Silicone Polymers	7
2.2.1 Polysiloxanes	8
2.2.2 Nomenclature and Properties of Polysiloxanes	9
2.2.3 Synthesis of Polysiloxanes	12
2.3 Ring Opening Polymerization	14
2.3.1 Anionic Ring Opening Polymerization	14
2.3.2 Cationic Ring Opening Polymerization	16
2.4 Cross-linking of Polysiloxanes	18
2.4.1 Moisture Cure	19
2.4.2 Hydrosilylation	19
2.4.3 UV Cure	20
2.5 Catalysts	21

2.6	Lorentz-Lorenz Relationship	21
2.6.1	Mechanism of Light Interaction with Particles	21
2.6.2	Lorentz-Lorenz Law	23
2.7	Fractional Free Volume	26
2.8	Cross-link Density	26
2.9	Instruments Analysis	27
2.9.1	Fourier Transform Infrared Spectroscopy	27
2.9.2	Nuclear Magnetic Resonance Spectroscopy	28
2.9.3	Gel Permeation Chromatography	31
2.9.4	Thermogravimetric Analysis	33
2.9.5	Differential Scanning Calorimetry	33
2.9.6	Ultra Violet-Visible Spectrometry	34
2.9.7	Refractive Index Analysis	36
2.9.8	X-ray Diffraction	37
2.9.9	Durometer Shore A	39

CHAPTER 3: EXPERIMENTAL

3.1	Materials	41
3.1.1	Octamethylcyclotetrasiloxane	41
3.1.2	1,1,3,3-Tetramethyldisiloxane	41
3.1.3	Octaphenylcyclotetrasiloxane	42
3.1.4	2,4,6,8-Tetramethyl-2,4,6,7-tetravinylcyclotetrasiloxane	42
3.1.5	Platinum (0)-1,3-vinyl-1,1,3,3-tetramethylsiloxane	43
3.1.6	Trifluoromethanesulfonic acid	43
3.1.7	Triarylsulfonium hexafluoro antimonate salts	43
3.1.8	2-Hydroxy-2-methyl-1-phenyl-propan-1-one	44
3.1.9	Iodonium, (4-methylphenyl) [4-(2-methylpropyl)phenyl hexafluorophosphate	44
3.1.10	Diethyl ether	45
3.1.11	Magnesium sulphate	45
3.1.12	Potassium hydroxide	45
3.1.13	Toluene	45
3.2	Synthesis	45

3.2.1	Synthesis of series one	46
3.2.1.1	Synthesis of hydrosilyl-terminated polydimethylsiloxane prepolymers	46
3.2.1.2	Hydrosilylation of hydrosilyl-terminated PDMS with 2,4,6,8-tetramethyl-2,4,6,8-tetravinylcyclotetrasiloxane	48
3.2.1.3	Thermal curing of S1	48
3.2.1.4	Ultra Violet curing of S1	48
3.2.2	Synthesis of series two	49
3.2.2.1	Synthesis of polydimethylsiloxane-co-polydiphenylsiloxane	49
3.2.2.2	Synthesis of hydrosilyl-terminated polydimethylsiloxane -co-polydiphenylsiloxane prepolymers	50
3.2.2.3	Hydrosilylation of hydrosilyl-terminated polydimethylsiloxane-co-polydiphenylsiloxane Prepolymers with 2,4,6,8-tetramethyl-2,4,6,8-tetravinylcyclotetrasiloxane	51
3.2.2.4	Thermal curing of S2	52
3.3	Characterization	52
3.3.1	Fourier Transform Infrared Spectroscopy	52
3.3.2	Nuclear Magnetic Resonance Spectroscopy	52
3.3.3	Gel Permeation Chromatography	53
3.3.4	Density Measurement	53
3.3.5	Cross-link Density Measurement	53
3.3.6	Thermogravimetric Analysis	55
3.3.7	Differential Scanning Calorimetry	55
3.3.8	Ultra Violet-Visible Spectrometry	55
3.3.9	Refractive Index	56
3.3.10	X-ray Diffraction	56
3.3.11	Shore A Hardness	56

CHAPTER 4: RESULTS AND DISCUSSION

4.1	Series One	58
4.1.1	Synthetic Consideration	58
4.1.2	Structure Conformation	60
4.1.2.1	Fourier Transform Infrared	60
4.1.2.2	Nuclear Magnetic Resonance	62
4.1.2.2.1	¹ H-NMR	62
4.1.2.2.2	²⁹ Si-NMR	64
4.1.3	Thermal Properties	67
4.1.3.1	Thermogravimetric Analysis	67
4.1.3.2	Differential Scanning Calorimetry	68
4.1.4	Degree of Cross-link Network	70
4.1.5	Optical Properties	72
4.1.5.1	Ultra Violet- Visible Spectroscopy	72
4.1.5.2	Refractive Index	74
4.1.5.3	Fractional Free volume	76
4.1.6	X-ray diffraction	77
4.1.7	Hardness	79
4.2	Series Two	80
4.2.1	Synthetic Consideration	80
4.2.2	Structure Conformation	82
4.2.2.1	Fourier Transform Infrared	82
4.2.2.2	Nuclear Magnetic Resonance	84
4.2.2.2.1	¹ H-NMR Analysis	84
4.2.2.2.2	²⁹ Si-NMR Analysis	86
4.2.3	Degree of Cross-link Network	89
4.2.4	Thermal Properties	90
4.2.4.1	Thermogravimetric Analysis	90
4.2.4.2	Differential Scanning Calorimetry	92
4.2.5	Optical Properties	94
4.2.5.1	Ultra Violet-Visible Spectroscopy	94
4.2.5.2	Refractive Index	96
4.2.6	Hardness	97

4.3	UV Curing of the Series One	99
4.3.1	Curing Method	99
4.3.2	Structure Conformation	104
4.3.2.1	Fourier Transform Infrared	104
4.3.3	Degree of Cross-link Network	107
4.3.4	Thermal Properties	107
4.3.4.1	Thermogravimetric Analysis	107
4.3.4.2	Differential Scanning Calorimetry	109
4.3.5	Optical Properties	111
4.3.5.1	Ultra Violet-Visible Spectroscopy	111
4.3.5.2	Refractive Index	113
4.3.6	Hardness	114
CHAPTER 5: CONCLUSIONS AND RECOMMENDATIONS		116
5.1	Conclusions	116
5.2	Recommendations for Future Research	117
REFERENCES		118
APPENDICES		
A.1	Paper Journal of Advanced Materials Research (Published)	127
A.2	Paper Journal of Polymer International (Accepted)	128
A.3	Conference Proceeding 1- National Symposium on Polymeric Materials 2010 (NSPM 2010) Awana Porto Malai Resort Langkawi, Kedah.	129
A.4	Conference Proceeding 2- International Conference on Advanced Engineering Materials and Technology (ICAEMT 2011), Sanya, China.	130

LIST OF TABLES

		Page
Table 2.1	Structural unit of polysiloxanes (Noll, 1968).	9
Table 2.2	Properties of polysiloxanes.	12
Table 2.3	²⁹ Si-NMR chemical shift for polysiloxanes.	30
Table 3.1	Percentage of weight ratios (v/w) of raw material used in hydrosilyl-terminated polydimethylsiloxane (HTP) compounds.	47
Table 3.2	Summary of formulation used in synthesis of S2.	51
Table 4.1	Molecular weight and polydispersity of HTP samples of S1 at different end-capper percentages based on NMR and GPC.	66
Table 4.2	Thermal and swelling behaviour of S1 samples with different percentages of end-capper.	67
Table 4.3	Swelling behaviour of S1 samples with different percentages of end-capper.	70
Table 4.4	Refractive index (at 25°C), for S1 samples with different percentages of end-capper.	74
Table 4.5	Fractional free volumes (FFV) and dominant <i>d</i> - spacing (Å) for S1 samples with different percentages of end-capper.	77
Table 4.6	Molecular weight and polydispersity of S2-HTPCP samples at different P ₄ percentages based on GPC.	89
Table 4.7	Swelling behaviour of S2 samples with different phenyl content of P ₄ .	90
Table 4.8	Thermal behavior S2 samples with different percentages of P ₄ .	91
Table 4.9	The results and variation of parameters for UV curing.	100
Table 4.10	UV curing of hydrosilyl-terminated PDMS (HTP) using different percentage (%) amount of TSHFA photoinitiators.	103
Table 4.11	UV curing of hydrosilyl-terminated PDMS (HTP) with different curing time.	104

Table 4.12	Visual observation of the appearance of samples S1/UV after UV curing.	104
Table 4.13	Thermal behaviour of sample S1-30% and S1/UV-30%.	109

LIST OF FIGURES

	Page
Figure 1.1	Schematic of a 5 mm indicator LED (Segler, 2005). 2
Figure 2.1	Representative structure of three major categories silicone polymers (Frank et al., 2005). 7
Figure 2.2	A schematic represent of polysiloxanes linkages form from hydrolysis of the chloride (Ravve, 2000). 8
Figure 2.3	Four common functional groups of polysiloxanes (M. Bogdan & Julian, 1995). 8
Figure 2.4	The nomenclature of siloxanes (Chandrasekhar, 2005). 10
Figure 2.5	The hybrid nature of the silicone polymer (Frank et al., 2005). 10
Figure 2.6	Hydrolysis of dimethyldichlorosilane (Jones et al., 2001). 12
Figure 2.7	Hydrolysis of dimethyldichlorosilane yield linear and cyclic siloxanes (Chojnowski et al., 1987) . 13
Figure 2.8	The condensation of silanos to polymeric products is catalysed by both acids and bases (Saunders, 1973). 14
Figure 2.9	General ring opening polymerization equation (Jones, 2000). 14
Figure 2.10	Reaction mechanism during initiation, propagation and chain transfer in anionic ring-opening polymerization (Dubois et al., 2009). 16
Figure 2.11	General reaction mechanism during initiation, propagation and termination of cationic ring opening polymerization (Jones et al., 2001). 18
Figure 2.12	General reaction of moisture cure (Jones et al., 2001). 19
Figure 2.13	General reaction mechanism of hydrosilylation (Jones et 20

	al., 2001).	
Figure 2.14	Basic arrangement of NMR spectrometer (Abraham et al., 1988;Maimon et al., 2006).	28
Figure 2.15	Downfield and upfield in NMR spectrum.	29
Figure 2.16	Example of multiplet in ¹ H-NMR analysis.	30
Figure 2.17	The instrumentation of GPC (Skoog et al., 2007).	32
Figure 2.18	Schematic of TGA instrument (Brown & Gallagher, 2007).	33
Figure 2.19	Principal of DSC instrument (Jackson & Hargreaves, 2009).	34
Figure 2.20	Single beam UV-Visible Spectrometer used to determine the absorbency (Rabilloud, 2000).	35
Figure 2.21	Cross section of part of the optical path of an refractometer (Hanson, 2006).	36
Figure 2.22	Schematic of X-ray diffraction (He, 2011).	39
Figure 2.23	(a) Shore A durometer; (b) Shore D durometer (Qi et al., 2003).	40
Figure 3.1	Chemical structure of octamethylcyclotetrasiloxane (D ₄).	41
Figure 3.2	Chemical structure of 1,1,3,3- tetramethyldisiloxane (TMDS).	41
Figure 3.3	Chemical structure of octaphenylcyclotetrasiloxane (P ₄).	42
Figure 3.4	Chemical structure of 2,4,6,8-tetramethyl-2,4,6,8 tetravinylcyclotetrasiloxane (D ₄ V).	43
Figure 3.5	Chemical structure of Platinum(0)-1,3-vinyl-1,1,3,3-tetramethylsiloxane.	45

Figure 3.6	Chemical structure of triarylsulfonium hexafluoroantimonate salts, mixed, 50wt% in propylene carbonate.	44
Figure 3.7	Flow chart of an overview of the methodologies.	46
Figure 4.1	A schematic reaction of cross-linked network of the product S1.	59
Figure 4.2	Proposed cross-linked network (not to scale) between D ₄ V with HTP. The bold square structure refer to the D ₄ V acting as anchorage for cross-linked network for HTP linear chains.	60
Figure 4.3	FTIR spectrum of the D ₄ , TMDS, D ₄ V and completion the hydrosilylation process of S1-30%.	63
Figure 4.4	¹ H-NMR spectrum of S1-30% HTP in CDCl ₃ .	64
Figure 4.5	²⁹ Si-NMR spectrum of S1-30% HTP.	65
Figure 4.6	Solid ²⁹ Si-NMR spectrum of S1-30% cured.	65
Figure 4.7	TGA for thermal decomposition of S1 with different percentage of end-capper.	68
Figure 4.8	DSC trace for thermal glass transition temperature (T _g) of S1 series derived from PDMS with different percentages of end-capper in nitrogen atmosphere.	69
Figure 4.9	Cross-link density and swelling behaviour of the S1 samples for 30%, 40% and 50% (v/w) in toluene.	71
Figure 4.10	The UV-Vis transmittance spectroscopy of S1 series.	73
Figure 4.11	FTIR spectrum of the S1-50% before and after cured.	73
Figure 4.12	Plot of $n^1 - 1/n^2 + 2$ versus density of S1 samples.	75

Figure 4.13	Repeat unit for polysiloxane network used to determine FFV, where $n = 15, 16, 22, 18$ and 14 for 10%, 20%, 30%, 40% and 50% (v/w) end-capper respectively.	76
Figure 4.14	X-ray diffraction data of S1 samples with different percentage of end-capper.	78
Figure 4.15	Shore A hardness of S1 samples with different percentage of end-capper.	79
Figure 4.16	A schematic reaction of the synthesis mechanism of the S2 product.	81
Figure 4.17	FTIR spectrum of copolymer of D ₄ and P ₄ in series 2.	83
Figure 4.18	FTIR spectrum showing the completeness of the hydrosilylation process of S2-30%.	85
Figure 4.19	¹ H-NMR spectrum of S2-30% HTPCP in CDCl ₃ .	86
Figure 4.20	²⁹ Si-NMR spectrum of S2-30% HTPCP.	87
Figure 4.21	Solid state ²⁹ Si-NMR spectrum of S2-30%.	88
Figure 4.22	Cross-link density and swelling behaviour of the S2 samples for 10%, 20% and 30% (v/w) in toluene.	90
Figure 4.23	TGA for thermal decomposition of S2 with different percentage of P ₄ .	91
Figure 4.24	TGA for thermal decomposition of comparison between optimum S1 and S2.	92
Figure 4.25	DSC trace for thermal glass transition temperature (T _g) of S2 series with different phenyl content in nitrogen atmosphere.	93
Figure 4.26	Comparison of DSC trace for thermal glass transition temperature T _g between S1-30% and S2-30%.	93
Figure 4.27	The UV-Vis transmittance spectroscopy of S2 series.	95

Figure 4.28	The UV-Vis transmittance of comparison between optimum S1 and S2.	95
Figure 4.29	Refractive index of system S2 with different percentage of phenyl content.	96
Figure 4.30	Comparison of refractive index between samples Series 1 and series 2.	97
Figure 4.31	Shore A hardness of S2 samples with different phenyl content of P ₄ .	98
Figure 4.32	Shore A hardness of comparison between sample S1-30% (series one) and S2-30% (series two).	98
Figure 4.33	A schematic represent reaction of TSHFA photoinitiator to generate reactive species.	100
Figure 4.34	Mechanism of UV-photopolymerization for series S1/UV.	101
Figure 4.35	Mechanism of UV curing for series S1/UV.	102
Figure 4.36	FTIR spectrum of D ₄ , TMDS, D ₄ V and completion the hydrosilylation process of S1/UV-30%.	106
Figure 4.37	Cross-link density and swelling behaviour of the S1/UV samples for 30%, 40% and 50% (v/w) in toluene.	107
Figure 4.38	TGA for thermal decomposition of S1/UV-30% (UV curing) with S1-30% (thermal curing) samples.	108
Figure 4.39	DSC traces for glass transition temperature T _g of S1/UV series in nitrogen atmosphere.	110
Figure 4.40	Comparison of DSC trace for glass transition temperature T _g between thermal curing and UV curing of S1-30% end-capper.	110
Figure 4.41	The UV-Vis transmittance spectroscopy of S1/UV series.	111

Figure 4.42	Comparison of the UV-Vis transmittance spectroscopy between thermal curing and UV curing of S1-40%.	112
Figure 4.43	Refractive index of system S1 with UV curing.	113
Figure 4.44	Comparison of refractive index between sample S1-40% (thermal curing) and S1/UV-40% (UV curing).	114
Figure 4.45	Shore A hardness of S1/UV samples with different percentage of end-capper after UV curing.	115
Figure 4.46	Shore A hardness of comparison between sample S1-40% (thermal curing) and S1/UV-40% (UV curing).	115

LIST OF ABBREVIATIONS

ASTM	American Society for Testing and Materials
AROP	Anionic ring opening polymerization
CROP	Cationic ring opening polymerization
D ₄	Octamethylcyclotetrasiloxane
DSC	Differential Scanning Calorimetry
D ₄ V	2,4,6,8-tetramethyl-2,4,6,8-tetravinylcyclotetrasiloxane
FFV	Fractional free volume
FTIR	Fourier Transform Infrared
GPC	Gel Permeation Chromatography
H	Hydrogen
H-NMR	Proton Nuclear Magnetic Resonance
HTP	Hydrosilyl-terminated polydimethylsiloxane
HTPCP	Hydrosilyl-terminated polydimethylsiloxane-co- polydiphenylsiloxane
KOH	Potassium hydroxide
LED	Light emitting diodes
Me	Methyl
MgSO ₄	Magnesium sulphate
MW	Molecular weight
MWD	Molecular weight distribution
N ₂	Nitrogen gas
P ₄	Octaphenylcyclotetrasiloxane
PDMS	Polydimethylsiloxane

Ph	Phenyl
Pt	Platinum
RI	Refractive index
S1	Series one under thermal curing
S1/UV	Series one under UV curing
S2	Series two containing P ₄ under thermal curing
T	Transmittance
TFSA	Trifluoromethanesulfonic acid
THF	Tetrahydrofuran
TGA	Thermogravimetric Analysis
TMDS	1,1,3,3-tetramethyldisiloxane
TSHFA	Triarylsulfonium hexafluoro-antimonate salts
UV	Ultra Violet
UV-Vis	Ultra Violet Visible
V _{vdw}	Volume occupied by the atoms on van der Waal radii
XRD	X-ray Diffraction

LIST OF SYMBOLS

%	Percentage
>	More than
<	Less than
\geq	More than or equal to
\pm	Tolerance
$^{\circ}$	Degree
$^{\circ}\text{C}$	Degree Celsius
$^{\circ}\text{F}$	Degrees Fahrenheit
$^{\circ}\text{C min}^{-1}$	Degree Celsius per minute
\AA	Angstrom
ρ	Density
α	Polarizability
ϵ	Dielectric constant
θ	Theta
cm	Centimetre
cm^{-1}	Wave number
h	Hour
Hz	Hertz
g	Gram
g/cm^3	Gram per centimetre cube
gcm^{-1}	Gram per centimetre
g/mL	Gram per millilitre
gmol^{-1}	Gram per mole

mol/cm ³	Mole per centimetre cube
MHz	Mega Hertz
min	Minute
mg	Milligram
mL	Millilitre
mm	Millimetre
mmHg	Millimetre of mercury
MPa	Mega pascal
n	Repeated unit n
<i>n</i>	Refractive index
N	Avogadro's number
nm	Nanometre
ppm	Part per million
rpm	Rotation per minute
s	Second
T _g	Glass transition temperature
wt%	Weight percent
<i>v</i>	Volume
v/w %	Volume per weight percentage

SINTESIS DAN SIFAT-SIFAT BAGI POLISILOKSANA PAUTAN SILANG SANGAT TINGGI UNTUK PENGKAPSULAN LED

ABSTRAK

Kajian ini memfokuskan pada dua siri sintesis polisiloksana. Siri pertama (S1) adalah hidrosilil dengan penamat polidimetilsiloksana (HTP) dimatangkan dengan 2,4,6,8-tetrametil-2,4,6,8-tetravinil siklotetrasiloksana (D_4V) dan siri kedua (S2) adalah menggabungkan oktafenilsiklotetrasiloksana (P_4) ke dalam siri pertama. Kedua-dua siri polimer menjalani pematangan terma. Pematangan UV telah dilakukan pada siri pertama untuk mengurangkan masa pematangan serta membandingkan sifat-sifat mereka. Produk polisiloksana adalah berbentuk gel yang jelas. Ciri elastomer siri S1 adalah bergantung kepada kepekatan terminal rantai iaitu 1,1,3,3-tetrametildisiklosana manakala siri S2 adalah bergantung kepada jumlah kumpulan fenil daripada oktafenilsiklotetrasiloksana (P_4) dalam sintesis. Struktur kimia polimer telah dibuktikan oleh FTIR dan analisis NMR manakala taburan berat molekulnya ditentukan oleh GPC. Sifat-sifat terma ditentukan oleh TGA dan DSC manakala ciri-ciri optik polimer ini ditentukan dengan ukuran indeks biasan dan serapan UV. Ketumpatan pautan silang ditentukan dengan ujian pembengkakan dan kekerasan polimer pula ditentu oleh Shore durometer A. Sampel S1-30% dalam siri pertama telah didapati memberi kesan keliatan optimum. Polimer berasaskan siloksana ini mempunyai T_g dalam julat $-110\text{ }^\circ\text{C}$ sampai $-120\text{ }^\circ\text{C}$ dan mempunyai kestabilan terma yang sangat baik dengan suhu penguraian $600\text{ }^\circ\text{C}$. Bahan tersebut juga memaparkan indeks biasan yang sangat tinggi and sesuai untuk kegunaan sebagai penglitup LED. Ciri-ciri optik, sifat-sifat terma dan mekanikal adalah berkait rapat dengan ketumpatan pautan silang. Kesan nisbah isipadu bebas dan 'penumpatan' rangkaian telah dijelaskan dan didapati menyumbang kepada pergantungan ini. Model Lorentz-Lorenz telah digunakan untuk menyokong pemerhatian ini.

SYNTHESIS AND PROPERTIES OF HIGHLY CROSS-LINKED POLYSILOXANE FOR LED ENCAPSULANT

ABSTRACT

The research focuses on the synthesis of two series of polysiloxane. The first series (S1) is hydrosilyl-terminated polydimethylsiloxane (HTP) that was cured with 2,4,6,8-tetramethyl-2,4,6,8-tetravinyl cyclotetrasiloxane (D_4V) and second series (S2) is the incorporation of octaphenylcyclotetrasiloxane (P_4) into first series. The polymers of both series underwent thermal curing. UV curing was performed on the first series to improve the curing time as well as comparing their properties. The polysiloxanes product was a water clear gel form. The elastomeric feature of series S1 was dependent on the end-capper concentration, 1,1,3,3-tetramethyldisiloxane while series S2 was dependent on the amount of phenyl group of octaphenylcyclotetrasiloxane (P_4) employed during its synthesis. FTIR and NMR was used to confirm the functional group of HTP and completion of the hydrosilylation reaction. TGA was used to measure the residue mass of samples S1 and S2, while DSC was used to find the T_g of cross-linked samples. UV transmittance analysis was used to measure the transparency of the samples. Atago refractometer was used to measure the refractive index of the samples. Lastly, the swelling test was used to estimated crosslink density of samples and Shore A durometer was used to measure the hardness of samples. End-capper concentration of 30% (v/w) in first series was found to affect the optimum toughness of the product. The siloxane-based polymer displayed T_g in the range of $-110\text{ }^\circ\text{C}$ to $-120\text{ }^\circ\text{C}$ and with excellent thermal stability where decomposition temperature was around $600\text{ }^\circ\text{C}$. The materials also displayed refractive index of 1.4 – 1.5 which is within an acceptable range of application as electronic devices encapsulant. Series 2 shows higher optical, thermal and mechanical properties compared to series 1. These optical, thermal and mechanical properties were closely related to the cross-link density. The effect of fractional free volume and ‘densification’ of the network was elucidated and found to contribute to this dependency. Lorentz-Lorenz model was used to support these observations.

CHAPTER 1

INTRODUCTION

1.1 Introduction

Light Emitting Diodes (LEDs) have been extensively investigated as the potential next generation technology for flat panel display and lighting to replace incandescent, fluorescent, and neon lamps (Mott et al., 1990). This is due to their ability to produce high luminosity at low voltages, longer service life, lower cost, flexible displays and their compatibility with silicon-integrated circuits (Skal and Shklovskii, 1975; Kumar et al., 2006). Currently, due to the tremendous development in optoelectronic market, continuous improvement and enhancement of the light-emitting efficiency of LEDs demand to meet the high brightness challenge. Basically, LEDs are solid-state semi-conductor devices that convert electrical energy directly into light. LED generation of light leads to high efficacy because most of the energy radiates within the visible spectrum (Tarsa and Thibeault, 2002). LEDs can be extremely small and durable. They also provide longer lamp life than other sources. The LED encapsulant and the lead frame occupy most of the volume of the whole electronic. The light generating chip is quite small, typically 0.25 millimeters square. LED chip is a solid crystal material. Light is generated inside the LED chip when current flows across the junctions of different materials (Dasgupta et al., 2003).

Typically, LED encapsulant is made from a thin film to cover and protect the semiconductor substrate, cathode and anode from moisture, adverse environmental conditions and physical damage (Li et al., 2008). Nevertheless, the encapsulant must be homogenous, high optical transparency leading to the generation of sufficient light emission.

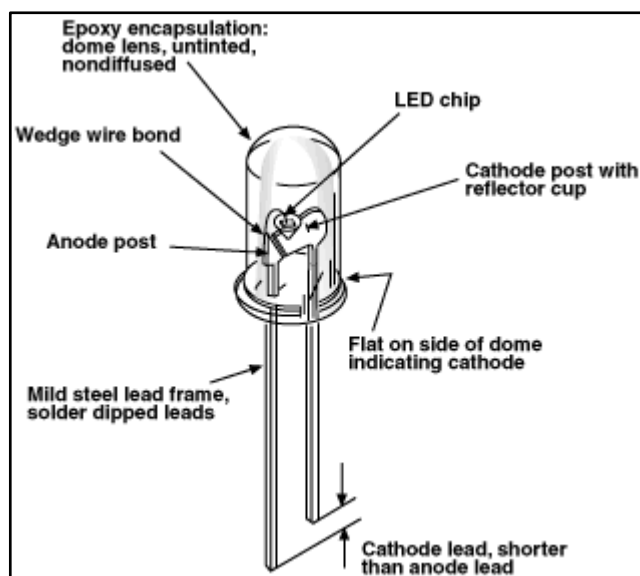


Figure 1.1: Schematic diagram of a 5 mm indicator LED (Segler, 2005).

In the recent years, many studies and researches have been performed on the thermal and optical improvement of LED encapsulant. In order to meet the demanding requirement for the production of LED encapsulant, many materials have been utilized especially polymer. Polymers have provided the opportunity for low cost and low or room temperature processing. A variety of polymer systems have been investigated with varying degrees of success (Hsu et al., 2012; Kim et al., 2012). One of those polymers is polysiloxanes.

Polysiloxanes have many desired properties when being considered for use in optoelectronic device applications. These is due to this material display high refractive index, transparency, good environmental stability, excellent thermal stability and moisture repelling capability (Li et al., 2008; Tai et al., 2001).

The refractive index can vary from 1.38 to 1.53 in commercially available materials, depending on the type of substituent groups. An epoxy-modified polysiloxane can be fabricated through the incorporation of epoxy group at the terminal of the polymer chain as an epoxy pendant groups (Jang and Crivello, 2003). This hybrid polymer combined the advantages of both epoxy and siloxane polymer.

The crosslink density depends on the number of epoxy groups in the polymer and this will account for the mechanical and hardness performance of the polymer. Besides that, epoxy-modified polysiloxane is also noted for its excellent thermal stability and their onset of thermal decomposition appeared at 300-350°C (Morita, 2005). This thermal stability can reduce the effect of thermal discoloration.

1.2 Problem Statement

The development in LED technology not only just involves miniaturization but also the need for high brightness. Conventional epoxy LED encapsulants are unable to fulfill the requirements as they are relatively brittle and tend to degrade or discolor in the exposure of radiation or high temperature. The discoloration of epoxy encapsulant becomes the one of the primary concern because it decreases the light output during LED operation.

Polysiloxanes provide several advantages over epoxy encapsulant as LED encapsulant, since polysiloxanes possesses many outstanding mechanical, thermal, and electro-optical properties, which have led to their wide use in various applications. A refractive index close to 1.70 is desirable in order to be compatible with the LED dies (Edwards and Zhou, 2001).

The issue of refractive index and transparency has been a major concern in the research involving polysiloxanes as LED encapsulant. Houghman et al. (1996) states that a reduction in free volume induced an increased in refractive index. Two factors affect the refractive index namely group polarizability and free volume. Aromatic structure displays a high group polarizability hence introducing a phenyl ring significantly affects an increase in refractive index. Free volume can be affected by inducing densification through cross-link network. By increasing cross-link

network, densification effect can be enhanced thus controlled the refractive index of material.

1.3 Research Objectives

This study is concerned with the refractive index of the LED encapsulant based on polysiloxane network. The objectives of the present study were:

- ❖ To prepare 2,4,6,8-tetramethyl-2,4,6,8-tetravinylcyclotetrasiloxane (D₄V) to tailor made a highly cross-link polysiloxane network.
- ❖ To study the effect of cross-link network on physical, optical, thermal and mechanical properties of the synthesized polysiloxane. .
- ❖ To study and compare phenyl incorporate polysiloxane and UV curing on cross-link polysiloxane network.

CHAPTER 2

LITERATURE REVIEW

2.1 Light Emitting Diode

2.1.1 Introduction

Light emitting diode (LED) technology has rapidly changed for over 35 years old. Improvements in the LED technology have stimulated new device applications. The worldwide production of LEDs is now around 4 billion units a month. Ten years ago, Japan was the principal LED producer, and Taiwan's output was a little over 10% of the world's demand. According to the ITIS (Industrial Technology Information Service) of Taiwan, Taiwan now produces around half the world's demand from its more than 30 LED manufacturers; Japan and the USA are recorded as the next most productive LED manufacturers. A LED device (Figure 1.1) consists of a semiconductor device encapsulated by a transparent and uniform thickness material to provide a uniform light emission (Lowery, 1999). The encapsulant is configured in a dome shape and acting as a lens for the emitted light (Mottier, 2010).

2.1.1.1 LED Encapsulants

LED encapsulants are transparent materials which provide optimal protection of LEDs. Materials of LED encapsulants are designed to endure higher operating temperatures, resist yellowing, and transmit more light than competing technologies. Besides that, they need to give better clarity at higher temperatures. LED lightings have to keep brighter over time and provide optimal LED protection. However, the encapsulants must be soft or resilient enough in the vicinity of the LED chip, so that mechanical stress does not damage the LED chip or the wire leads compromised

during thermal excursions or normal operating environments (Carey et al., 2001a).

The desired criteria of LED encapsulants are:

- Enhance light transmittance to increase the efficient traversing of light through LED encapsulants.
- Resist heat induced yellowing to reduce the degradation of heat and thermal cycle. Raise the performance and increase lifetime of LED encapsulants.
- Optically clear enough to let the light pass through the LED encapsulants without dispersion.
- UV-visible light cure in seconds to reduce cut process costs, decrease pollution and save energy.

Traditionally, materials used for LED encapsulants are made from epoxy, polymethylmethacrylate (PMMA), glass polycarbonate, optical nylon, polyurethane, UV doming resins or polybutadiene. However, these materials suffer from the drawback that their optical transmissive characterization degrade over time (Carey et al., 2001b). Nowadays, LED encapsulants are well developed to replace the conventional materials for example, epoxy incorporate with polysiloxane. Polysiloxanes have been selected as the encapsulants due to their high reliability under qualification stresses, non-yellowing, low ionic impurity, crack resistant, and the refractive index materials can customize up to 1.6 give excellent transparency into high frequency ranges. The LED dies is encapsulated with one or more silicone compounds, including a hard outer shell, an interior gel or resilient layer, or both. The silicone material is stable over temperature and humidity ranges, and over exposure to ambient UV radiation (Carey et al., 2001b).

2.2 Silicone Polymers

Silicone polymers are semi-inorganic materials and very important to electronic industry (Ravve, 2000). They are stable from -70 to 260 °C temperatures and outstanding mechanical, thermal, and electro-optical properties. Silicone polymers usually used as lubricants, adhesives, coatings, synthetic rubber and electronic devices, such as LED encapsulants, transistors, integrated circuits and computer chip (Mittal and Pizzi, 2009). Silicone polymers are divided into three major categories: fluids, resins, and elastomers (Frank et al., 2005). Figure 2.1 shows the representative structure of three major categories of silicone polymers.

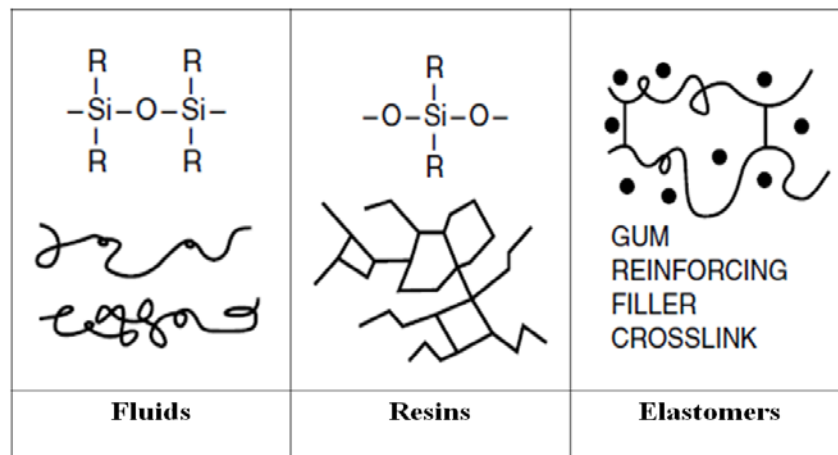


Figure 2.1: Representative structure of three major categories of silicone polymers (Frank et al., 2005).

Although silicone polymers are expensive, using the standard set by organic polymer had a remarkable commercial success. They are widely used as a host of the different industries for a broad variety of applications (Lane and Burns, 1996). Their popularity is due to (Brook, 2000) :

- i. Their properties, which cannot be matched by organic replacements; and
- ii. The fact that only small amounts of material are frequently required to achieve the desired result

2.2.1 Polysiloxanes

Polysiloxanes are heterochain polymers which have a backbone of alternating silicon and oxygen atoms, which are mixed inorganic-organic polymers with the two remaining valences of the silicon atoms linked to organic side groups (Muzafarov, 2010; Fried, 2003). Figure 2.2 shows the formation of polysiloxane linkages from hydrolysis of the halides, where R can be methyl, ethyl, or phenyl group. The products of hydrolysed silanols, are unstable and self condensed (Ravve, 2000).

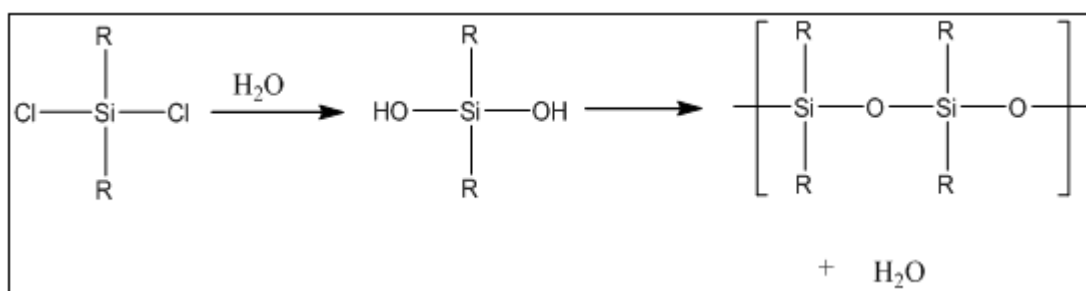


Figure 2.2: A schematic representation of polysiloxanes linkages from hydrolysis of chloride (Ravve, 2000).

Silicones can be synthesized with a wide variety of properties and compositions by varying the -Si-O- chain lengths, side groups, and cross-linking. This is illustrated in Figure 2.3. They can vary in consistency from liquid to gel to rubber and finally to hard plastic.

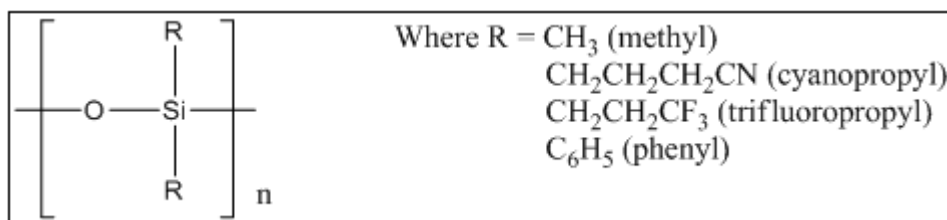


Figure 2.3: Four common functional groups of polysiloxanes (M. Bogdan and Julian, 1995).

Table 2.1 shows the structural unit of polysiloxanes. Monofunctional silanes such as R_3SiO form only disiloxane. In the mixtures R_2SiO_2 , $RSiO_3$ and SiO_4 , they also can work as terminators to end a chain. Bifunctional compounds such as R_2SiO_2 alone form chains and also cyclic siloxanes. The symbol “R” is alkyl group.

Table 2.1: Structural unit of polysiloxanes (Noll, 1968).

Structural formula	Composition	Functionality	Symbol*
R_3Si-O-	$R_3SiO_{1/2}$	monofunctional	M
$\begin{array}{c} R \\ \\ -O-Si-O- \\ \\ R \end{array}$	$R_2SiO_{2/2}$	difunctional	D
$\begin{array}{c} R \\ \\ -O-Si-O- \\ \\ O \\ \end{array}$	$RSiO_{3/2}$	trifunctional	T
$\begin{array}{c} \\ O \\ \\ -O-Si-O- \\ \\ O \\ \end{array}$	$SiO_{4/2}$	quadrafunctional	Q

* The symbols of M, D, T, and Q are used to represent mono, di, tri, and quadra functional siloxane monomers and polymers, respectively.

2.2.2 Nomenclature and Properties of Polysiloxanes

The silicone atom in polysiloxanes can be combined with one, two, or three organic groups and the remaining valences will be taken up by oxygen. By substituting a methyl group with -O-R into $Si(CH_3)_4$ as an example. It can assemble

polysiloxanes to form four types of structural units as shown in Table 2.1 (Noll, 1968; Chandrasekhar, 2005). Therefore, the structure of linear, branched, and cross-linked can be easily formed by polysiloxanes. Figure 2.4 shows the nomenclature of silicones.

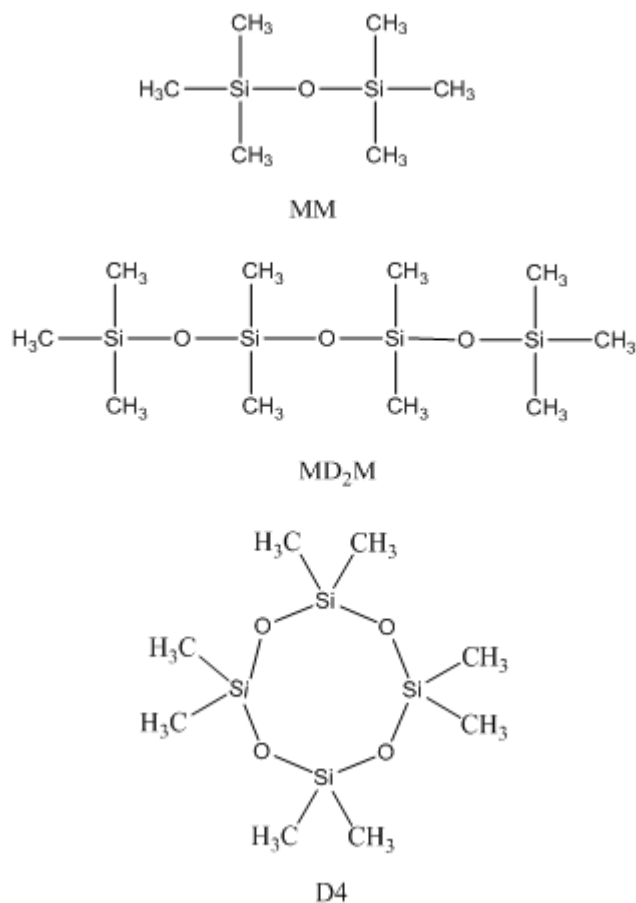


Figure 2.4: The nomenclature of siloxanes (Chandrasekhar, 2005).

Polysiloxane have many unique properties due to the free rotation of molecules along the Si–O and Si–C bond axes and the flexible nature of the siloxane backbone shown in Figure 2.5 (Frank et al., 2005).

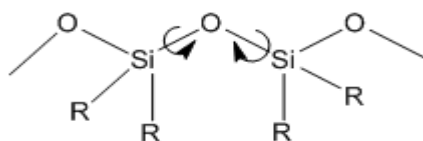


Figure 2.5: The hybrid nature of the silicone polymer (Frank et al., 2005).

Polysiloxanes have great flexibility chains due to the very low barrier free rotation of molecules along the Si–O and Si–C bond axes at 2.5 kJ mol^{-1} and the barrier of linearization of the Si-O-Si bond angle at 1.3 kJ mol^{-1} , which is shown in Figure 2.5 (Frank et al., 2005; Jones et al., 2001). The Si-O-Si bond has very large bond angle (145°) and low bending force constant (Ragheb and Riffle, 2010; Archer, 2001). As a result, the chains are very flexible and occupy a rather large volume, resulting in a high free volume in the material (Jaeger and Gleria, 2007). Larger intermolecular distance improves by the freedom of segmental chain motion and lowers down the intermolecular forces. This results in polysiloxanes having low modulus, high permeability, low glass transition temperatures (T_g) in the range of -70 to -150°C . The T_g of polysiloxanes depend on the substituent groups pendent to the main Si-O backbone chains (Dvornic, 2000; Flory et al., 1964). The T_g 's of polysiloxane, which reflect the ease of segmental motion along the chain, are very low, typically less than -120°C (Archer, 2001).

The high thermal and oxidative stability of polysiloxanes are due to the high Si-O bond strength as well as the partial ionic character of the Si-O bond (Voronkov et al., 1978). Such polymers are durable and resistant against temperatures up to 500°C (Put, 1998). Besides that, polysiloxanes are also transparent to visible and UV light as well as high resistance to ozone and corona discharge due to its stable polymer backbone (Noll, 1968; Voronkov et al., 1978). Polysiloxanes are known to possess exceptional hydrophobicity. This is due to two phenomena: (1) The methyl groups provide hydrophobic characteristics to the polymer; and (2) the flexibility of the silicone polymer backbone such that methyl groups may orient themselves at the interface (Owen et al., 1990). Table 2.2 shows the properties of polysiloxanes.

Table 2.2 : Properties of polysiloxanes (Harmon et al., 1992; Lotters et al., 1997).

Properties	Values
Refractive Index	1.5 – 1.7
Glass Transition Temperature	-150°C – -70°C
Hardness, Shore A	10 – 90

2.2.3 Synthesis of Polysiloxanes

There are two ways to synthesize linear polysiloxanes from silicone monomers, which are hydrolysis and polycondensation. The first step is a hydrolysis of the bifunctional silane precursor. However, the linear and cyclic oligomers obtained by hydrolysis process have too short chains for most applications (Jones et al., 2001). The second step is a transformation of oligomers into high molecular weight polymers either by a polycondensation of hydroxyl-ended, short chain polysiloxanes or by a ring opening polymerisation of the cyclic oligomers. With dimethyldichlorosilane, the hydrolysis reaction occurs according to general equation as shown in Figure 2.6.

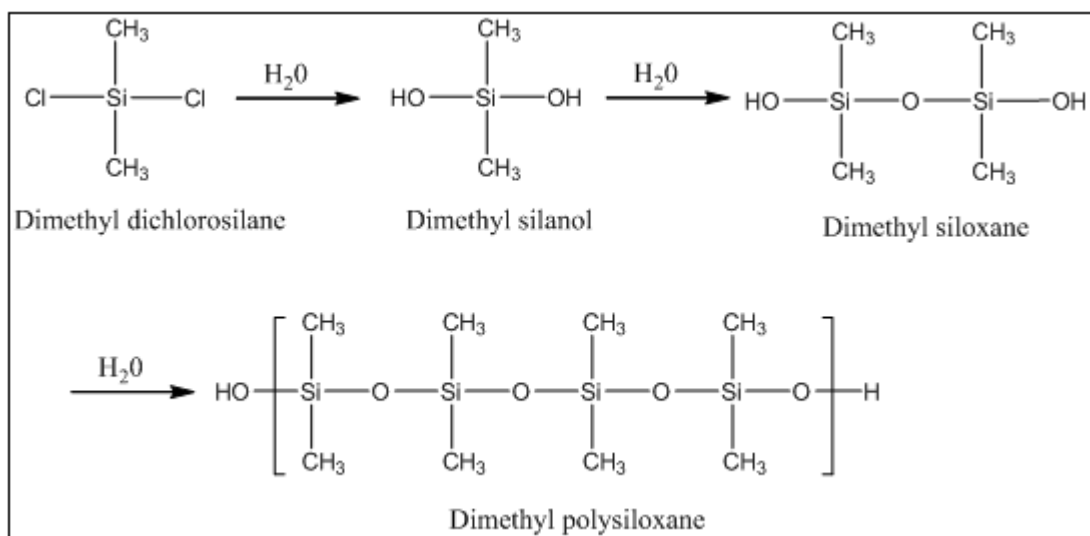


Figure 2.6: Hydrolysis of dimethyldichlorosilane (Jones et al., 2001)

The resulting dimethylsiloxane can be used as an end-capper for polymerization reactions to control the final molecular weight of the polysiloxane. The process may be performed either to give mainly cyclic siloxanes or linear hydroxyl-ended polydimethylsiloxane as shown in Figure 2.7 (Noll, 1968).

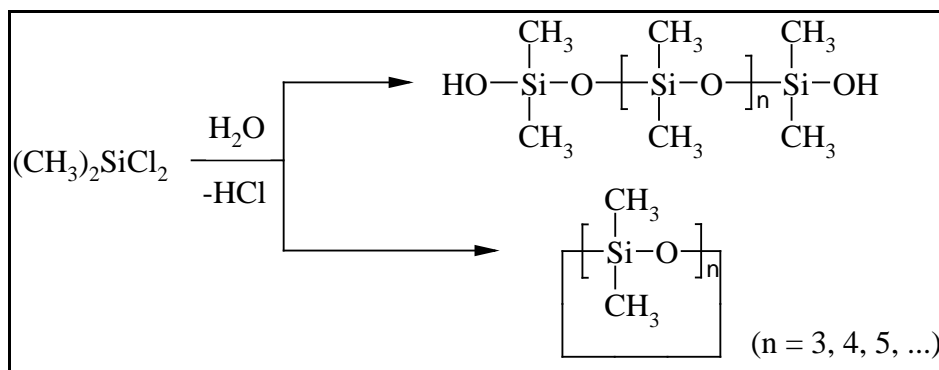
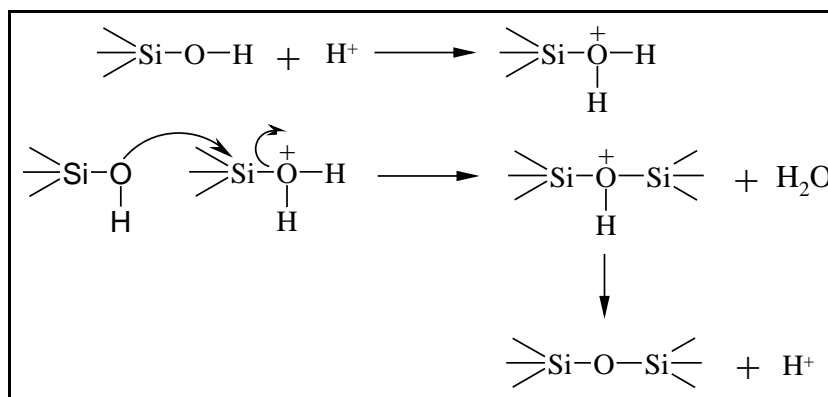
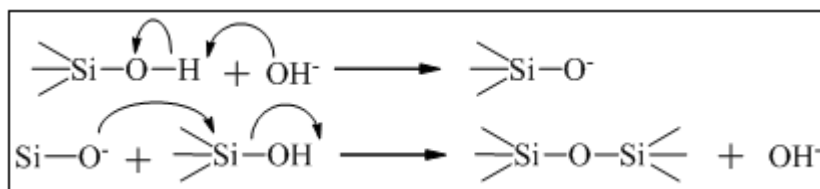


Figure 2.7: Hydrolysis of dimethyldichlorosilane yields linear and cyclic siloxanes (Chojnowski et al., 1987).

The condensation of silanols to form polymeric products is performed by both acid and base catalysts (Saunders, 1973). Acid catalysts are more efficient when the silanol carries electron-donating groups, whereas base catalysts when it carries electron-withdrawing groups. Some catalysts can induce redistribution by attacking the polymer chains with the formation of cyclic siloxanes (Jones et al., 2001). Figure 2.8 shows the example of acid-condensation and base-condensation reactions.



(a) Acid-catalyzed condensation:



(a) Base-catalyzed condensation:

Figure 2.8 : The condensation of silanols to polymeric products is catalysed by both acids and bases (Saunders, 1973).

2.3 Ring Opening Polymerization

Ring opening polymerization of cyclic siloxanes is a transformation process of the cyclosiloxane monomers into linear siloxane polymer through the cleavage of the Si-O-Si bond in the monomer ring and the subsequent reformation of the bond in the polymer chain as shown in Figure 2.9 (Jaeger and Gleria, 2007). This process has important advantages over the alternative polycondensation method, creating better conditions for the control of reactive end groups, hence a better control of molar mass (Dragan, 2006).

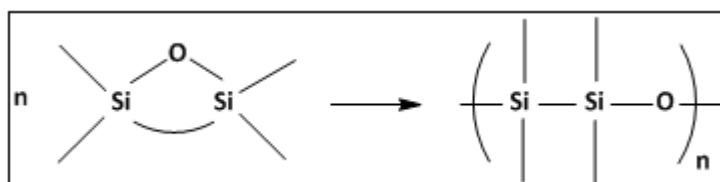


Figure 2.9: General ring opening polymerization equation (Jones, 2000).

Ring-opening polymerization can be carried out in either cationically or anionically condition. Both types of polymerization will be discussed, but only cationic ring opening polymerization was considered carried out in this project.

2.3.1 Anionic Ring Opening Polymerization

In anionic ring opening polymerization (AROP), strong inorganic, organic or organometallic bases are used as the initiators. Rings containing heteroatoms,

particularly oxygen, may be polymerized using anionic initiators. Alkali metal hydroxides such as KOH, tertiary ammonium and phosphonium and silanolate derived from them are common catalyst (Jones et al., 2001).

The reaction mechanism of (AROP) involved into three stages: initiation, propagation and termination (Warson and Finch, 2001). In initiation step, silanolate anion is formed. It acts as the active propagation centre which is capable of extending the polysiloxane chain by addition of monomers (Dubois et al., 2009). The propagation of reaction is continuous with monomers added to the polysiloxane backbone chain.

There will be no termination of AROP if there is no any protonic impurities and end-capper added to the system (Dubois et al., 2009). Thus, the reaction must be quenched to deactivate the silanolate centre and end the polymerization. Figure 2.10 shows the reaction mechanism during initiation, propagation, chain transfer and termination using end-capper (Jones, 2000).

The size of the counterion of catalyst is directly related to polymerization rate by increasing strongly in the series: $\text{Li}^+ < \text{Na}^+ < \text{K}^+ < \text{Rb}^+ < \text{Cs}^+$ (Jones et al., 2001). Lithium and sodium silanolate are not very powerful catalysts for cyclosiloxane polymerization unless used in conjunction with a solvent such as tetrahydrofuran (THF) or dimethyl sulfoxide (DMSO) (Patai et al., 2001). Cyclotrisiloxane has the highest reactivity due to its ring strain. As the size of monomer increases, the reactivity towards the silanolate ions increases too (Chojnowski, 1991). Figure 2.10 shows reaction mechanism during initiation, propagation and chain transfer in AROP.

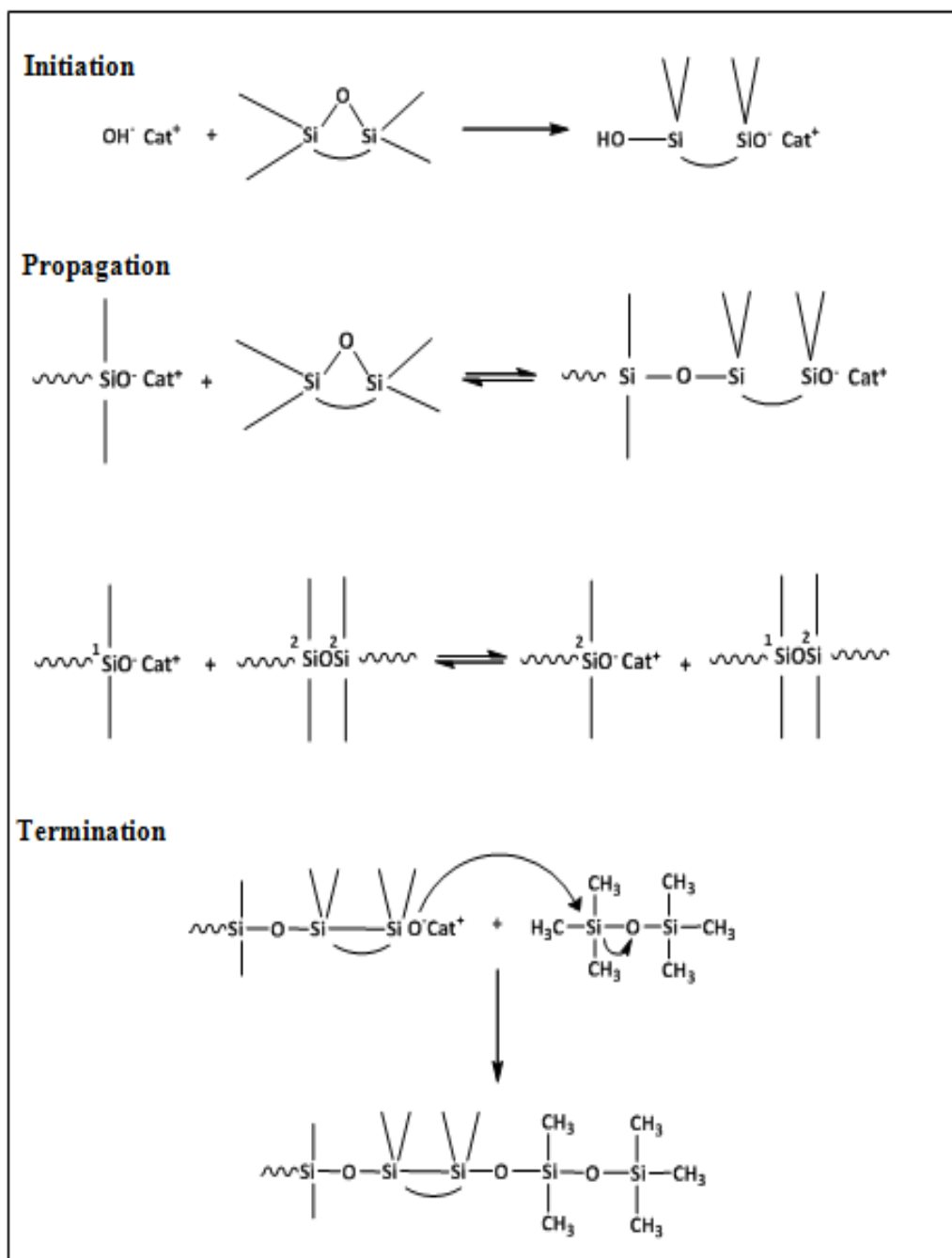


Figure 2.10: Reaction mechanism during initiation, propagation and chain transfer in anionic ring opening polymerization (Dubois et al., 2009).

2.3.2 Cationic Ring Opening Polymerization

Cationic ring opening polymerization (CROP) uses Bronsted and Lewis acid as catalysts. This includes strong protonic acid such as sulphuric acid, sulfonic acids, perchloric acid and a variety of Lewis acids such as ferric chloride, stannum chloride.

They are the common initiators for cationic polymerization of cyclosiloxanes (Jones et al., 2001). The advantage of this process is the relative insensitivity to acids of functional groups.

Compared to AROP, the reaction mechanism of the CROP of cyclosiloxane is very complex as shown in Figure 2.11. The tertiary siloxonium ions act as the active propagation centre to initiate the polymerization. The initiation step of CROP involves the splitting or acidolysis of the siloxane bond in a cyclic monomer to form reactive end groups. The reactive chain end will attack the siloxane bond in the cyclosiloxane monomers and then extending the polymer by adding monomers to the backbone chain in propagation step (Chandrasekhar, 2005; Brook, 2000). Termination step will be two types of condensation reaction. The first is the condensation of different reactive chain ends to form catalyst again, and the second type is the condensation of similar chain ends giving water as sub-product (Chojnowski and Cypryk, 2000).

The presence of contaminants such as water and silanols will affect the reaction rate. At higher water and silanol concentration, the polymerization is completely inhibited. From monomer aspect, the reactivity of the siloxane bond in cyclic siloxane oligomers varies with the size of ring and the type of substituent groups on silicon atom (Brook, 2000).

Compared to AROP, the molecular weight distribution (MWD) of polymer by CROP is relatively broad (1.6 to 2). It is because of the continuous initiation along the polymerization and also affect by the side reactions (condensation, back-biting and chain transfer). The contaminants such as water and alcohol are able to cleave the siloxane bond which is responsible for decreasing polymer molecular weight (Jones et al., 2001).

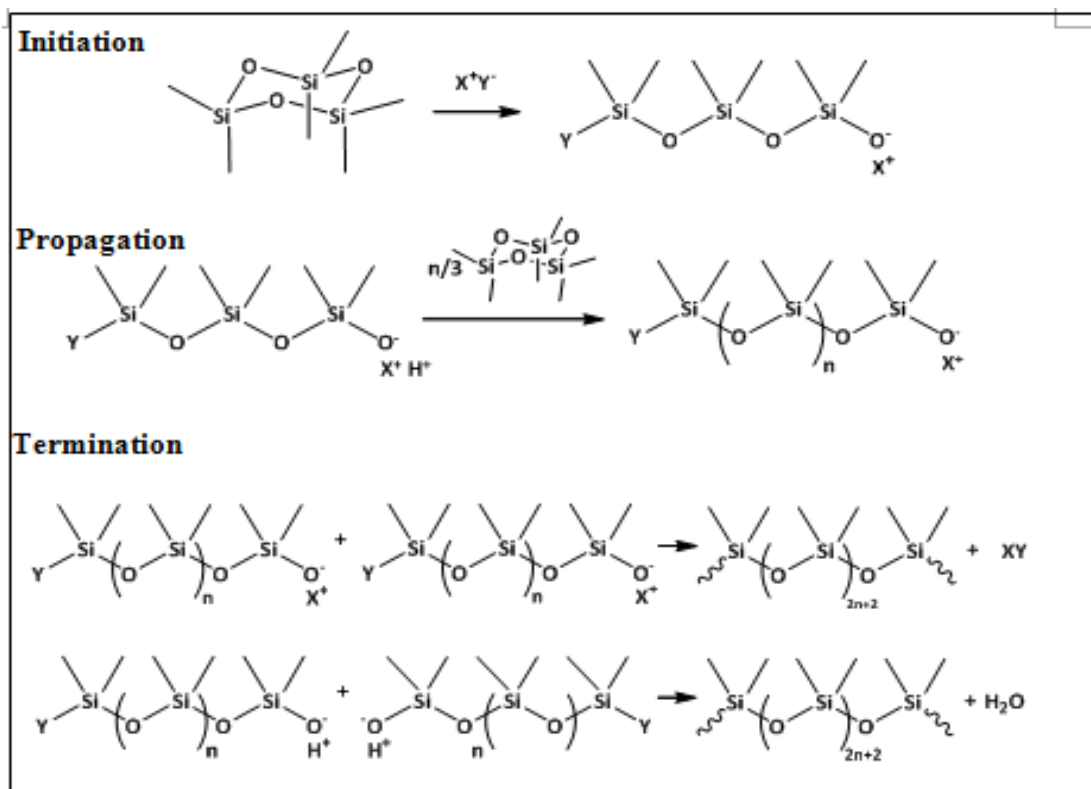


Figure 2.11: General reaction mechanism during initiation, propagation and termination of cationic ring opening polymerization (Jones et al., 2001).

2.4 Cross-linking of Polysiloxanes

Silicone fluids are valuable materials. However, many applications required the materials that do not flow. Thus, to form resins, coatings, and elastomers, it is necessary to cross-link the silicones. There are several possible routes to cross-linking that could be envisaged. However, the routes most commonly involve: (1) the incorporation of tri- or tetrafunctional silanes that can react in ionic conditions; or (2) the use of organic residues on the silicone polymers (methyl, vinyl, H groups) to form a network (Plueddemann, 1991). There are three different types of cross-linking: moisture cure (RTV), transition metal catalyzed hydrosilylation (typically platinum) or addition cure and UV cure.

2.4.1 Moisture Cure

Moisture curing (Figure 2.12) for single component systems is viscous adhesives that typically consist of non-volatile silicone prepolymers. These systems require moisture to trigger the curing reaction. Cured adhesives range from hard and rigid to soft and flexible depending on formulation. A major application for moisture curing silicone is the installation of windshields in automobiles. Recently, single component moisture curing polysiloxanes hot melts have been developed that combine the initial strength of hot melts with the improved heat resistance of moisture cured adhesives (Majumdar et al., 2011; Ren and Frazier, 2012). Cure is accomplished at room temperature via a reaction with moisture in air. Cure speed varies according to temperature and humidity and skin times range from 3 to 10 minutes.

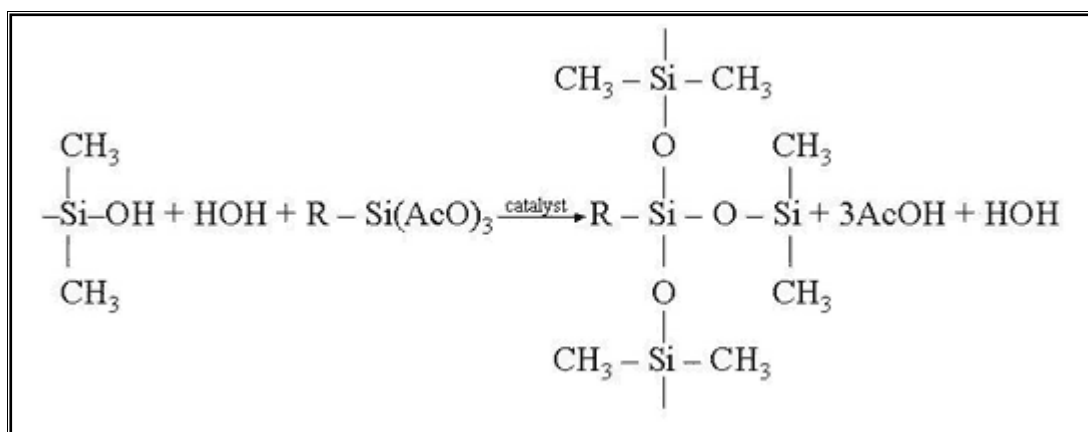


Figure 2.12: General reaction of moisture cure (Jones et al., 2001).

2.4.2 Hydrosilylation (Additional Cure)

Hydrosilylation is an addition reaction of hydrosilanes (Si-H) compounds to unsaturated bond, vinyl, CH₂=CH, or allyl, CH₂=CHCH₂, groups. Hydrosilylation of Si-H group with olefins, especially allyl derivatives, leads to a wide variety of functional silicones with a special organic reactivity (Patai et al., 2001). This reaction is one of the most efficient processes for making the silicon-carbon bond after the

direct process. It is also one of the methods of introduction of functionalized silanes (Si-Cl, Si-OR) or alkylsilanes to organic molecules in high yield (Marciniec, 2008). It allows for the functionalization of polysiloxanes with either hydride or vinyl-containing siloxane repeat units (Ragheb and Riffle, 2010).

The cross-linking complementary polymers that must be used are the silicone containing Si-H groups and the silicone is usually in a two-part system with the catalyst contained in the vinyl-polymer part (Marciniec, 2008). The reaction occurs rapidly and under very mild conditions (Figure 2.13). The onset temperature for hydrosilylation (ambient to 100°C) can be affected by changing the nature of catalyst and addition of specific inhibitors. There are no by products produced in the process, although residual platinum that remains trapped in the gel can turn the elastomer somewhat yellowish. The polymer can be cured via hydrosilylation reaction affording the desired cross-linking (Speier, 1979).

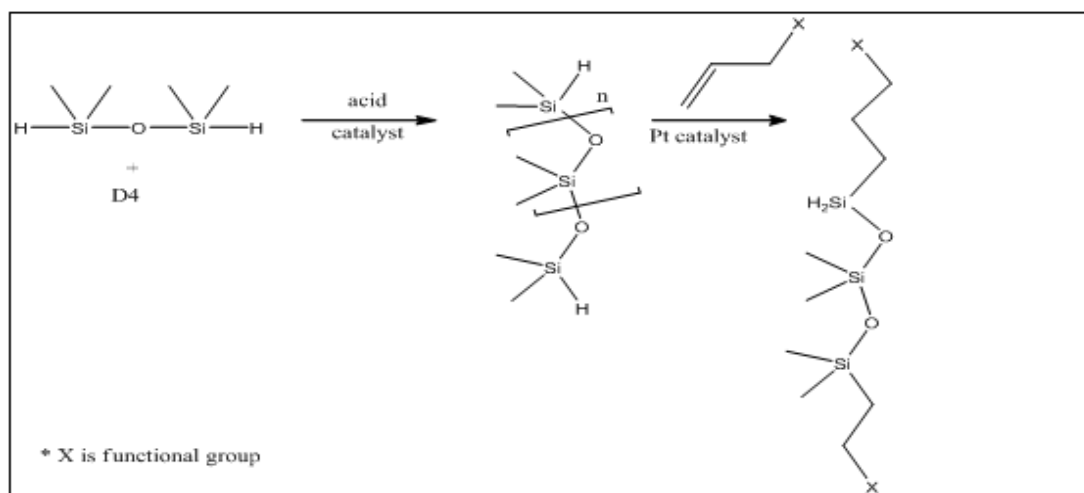


Figure 2.13: General reaction mechanism of hydrosilylation (Jones et al., 2001).

2.4.3 UV cure

Silicones do not readily undergo photodegradation. However, when under highly energetic radiations such as electron beam, gamma irradiation and intense UV, cross-linking can occur. When the silicone is simultaneously exposed to irradiation

in the presence of and oxygen, then the oxidation processes are accelerated, leading first to carbon oxidation, Si-C cleavage to give silanols, and silanol condensation to give cross-linking (Noll, 1968).

2.5 Catalysts

Catalysts are generally necessary to effect polymerization via equilibration (Chojnowski et al., 1987). Strong acids and bases catalyze both condensation and cleavage redistribution. Bronsted acids such as sulfuric acid, acid clay and triflic acid are frequently used as acidic catalysts. Although Lewis acids (TiCl_4 , $\text{Me}_3\text{SiOSO}_2\text{CF}_3$) will also initiate the polymerization, in the most cases a proton, formed from adventitious water by hydrolysis, is the active catalyst (Obriot et al., 1987). Hydroxide bases such as KOH, R_4NOH , and R_4POH efficiently catalyze polymerization under equilibrating conditions (Gilbert and Kantor, 1959).

Platinum catalyst is an efficient hydrosilylation catalyst (Speier, 1979). Under optimal conditions, catalyst concentrations of less than 1 ppm (part per million) are sufficient for complete a reaction. The reaction can be done in tetrahydrofuran, chloroform, and other chlorinated solvents, benzene, toluene and silicones (Ojima et al., 1998).

2.6 Lorentz-Lorenz Relationship

2.6.1 Mechanism of light interaction with particles

The Lorentz–Lorenz equation relates the refractive index of a substance to its polarizability (Born et al., 2000). The most general form of the Lorentz–Lorenz equation is

$$\frac{n^2 - 1}{n + 2} = \frac{4\pi}{3} N\alpha \quad (2.1)$$

where n is the refractive index, N is the number of molecules per unit volume, and α is the mean polarizability. It was independently formulated by Danish mathematician Ludvig Lorenz and Dutch physicist Hendrik Lorentz in 1878. The derivation of this equation involved the mechanism of interaction of electromagnetic radiation with particles which characteristically make up a material.

An electromagnetic wave is produced by a vibrating electric charge (Waldman, 2002) As the wave moves through the vacuum of empty space, it travels at a speed of c (3×10^8 m/s). Atoms are made up of electrons which vibrate at its natural or resonant frequency. When the wave impinges upon a particle of matter, the energy is absorbed and sets electrons within the atoms into vibration motion. If the frequency of the electromagnetic wave does not match the resonant frequency of vibration of the electron, there is a forced vibration with a small amount of energy being absorbed. Then the energy is reemitted in the form of an electromagnetic wave travelling at a new frequency. The newly emitted light wave continues to move through the interatomic space until it impinges upon a neighboring particle. The energy is absorbed by this new particle and sets the electrons of its atoms into vibration motion. And once more, if there is no match between the frequency of the electromagnetic wave and the resonant frequency of the electron, the energy is reemitted in the form of a new electromagnetic wave. This behavior corresponds to molecular scattering. The cycle of absorption and reemission continues as the energy is transported from particle to particle through the bulk of a medium. There will be a speed delay involved from c in the process of being absorbed and reemitted by the atoms of the material. An almost complete absorption will occur if the radiation frequency is equal to the resonant frequency. Subsequently, the net speed of an electromagnetic wave in any medium is somewhat less than its speed in a vacuum.

The index of refraction is the ratio of the speed of light in a vacuum (c) to the speed of light in the medium (v) (Waldman, 2002):

$$n = c/v \quad (2.2)$$

The governing factor affecting this change in speed is the electronic polarizability (Minges and Committee, 1989).

2.6.2 Lorentz-Lorenz Law

The basis of Lorentz–Lorenz equation is derived from the Clausius–Mossotti relation and Maxwell's formula which originate from the electronic behavior called electronic polarizability. In a unit volume, polarizability is given as

$$P = Nm \quad (2.3)$$

where N is number of dipoles per unit volume and m is dipole moment. Since polarization P is proportional to dipole moment m , the latter must be proportional to the electric field strength or $m = \alpha E$. Polarizability (symbol α) is a proportionality constant and is called polarizability. α is equal to the dipole moment induced in an atom or a molecule by an electric field of unit intensity and this value is typical of each different type of atom or molecules (Indulkar and Thiruvengadam, 2008). To a good approximation,

$$P = Nm = N\alpha E \quad (2.4)$$

The relation between polarizability with the permittivity of the dielectric material can be shown as:

$$\epsilon = 1 + \frac{N\alpha}{\epsilon_0} \quad (2.5)$$

where ϵ_0 is permittivity at vacuum. When a dielectric is placed in between two plate capacitor, the additional quantity of charged displaced per unit area is given by

$$D = D_0 + P \quad (2.6)$$

$$D = \epsilon_0 E + P \quad (2.7)$$

where D_0 is the initial charged displaced. From Equation 2.4,

$$D = E(\epsilon_0 + N\alpha) \quad (2.8)$$

Rearrangement will gives

$$D = \epsilon_0 \epsilon_r E \quad (2.9)$$

ϵ_r is the new permittivity. In gaseous state there is effectively no interaction between atoms. However in solid and liquids, there is interaction between atoms which give rise to the generation of local electric field known as Lorentz field, E_i . This field is not equal to the applied external field. So, the local dipole moment is given as

$$m = \alpha E_i \quad (2.10)$$

If there are N dipoles per m^3 then molar polarizability is given by

$$P = Nm = N\alpha E_i \quad (2.11)$$

Total charge in this system is equal to

$$D = \epsilon_0 E + N\alpha E_i \quad (2.12)$$

Equating this equation with that of Equation 2.9 will give

$$\epsilon_r = \frac{\epsilon_0 E + N\alpha E_i}{\epsilon_0 E} \quad (2.13)$$

$$\epsilon_r = 1 + \frac{N\alpha E_i}{\epsilon_0 E} \quad (2.14)$$

In order to determine permittivity of the dielectric material, ϵ_r , then E_i must be known. By taking approximation, μ

$$E_i = E + \frac{\mu}{\epsilon_0} P \quad (2.15)$$

where μ is a constant with the value of $1/3$ for isotropic material. So

$$E_i = E + \frac{P}{3\epsilon_0} \quad (2.16)$$